# CRITICAL HEAT FLUX AND PRESSURE DROP FOR A CANFLEX BUNDLE STRING INSIDE AN AXIALLY NON-UNIFORM FLOW CHANNEL

L.K.H. LEUNG, D.C. GROENEVELD, G.R. DIMMICK, D.E. BULLOCK AND W.W. INCH

Fuel Channel Thermalhydraulics Branch Chalk River Laboratories Atomic Energy of Canada Limited Chalk River, Ontario CANADA K0J 1J0

#### Abstract

Experimental data of dryout power and pressure drop have been obtained with a simulated string of twelve aligned, full-scale, CANFLEX® fuel bundles. The bundle string consisted of 43 elements and was equipped with junction and appendages simulations. It was installed inside three flow tubes simulating three different creep profiles: one had a uniform inside diameter of 103.86 mm and the other two had axially varying inside diameters, with a peak of either 107.29 mm or 109.16 mm (3.3% and 5.1% larger than the uniform tube). Pressure variations along the fuel string were obtained with differential-pressure cells connected to a number of pressure taps. Sliding thermocouples were used to obtain surface-temperature measurements and detect dryout. A wide range of steam-water flow conditions was covered in the current tests: an outlet-pressure range from 6 to 11 MPa, a mass-flow-rate range from 7 to 25 kg/s, and an inlet-fluid-temperature range from 200 to 290°C. This paper focuses primarily on data obtained at normal operating pressures with the axially non-uniform channel that had a maximum diameter 5.1% larger than the reference pressure tube.

Local and boiling-length-average (BLA) critical-heat-flux values were derived from the dryout-power data for various flow conditions. Unlike the traditional BLA approach, the averaging process was initiated from the onset of significant void (OSV), instead of from the saturation point. This allowed the extension of the BLA approach to subcooled dryout conditions. The OSV values were evaluated from the pressure distribution along the bundle string. Comparisons of various parameters were made between the 37-element and CANFLEX bundles. Overall, the dryout-power values were consistently higher for the CANFLEX bundle than the 37-element bundle. At inlet-flow conditions of interest, the dryout-power measurements were, on average, 17% higher for the CANFLEX bundle than the 37-element bundle. The fuel-string pressure drop was similar between the CANFLEX and 37-element bundle strings.

## 1. INTRODUCTION

A new design of the CANDU<sup>®(1)</sup> fuel bundle has recently been completed jointly by Atomic Energy of Canada Limited (AECL) and the Korea Atomic Energy Research Institute (KAERI), to deliver improved power and safety margins to reactor operators. It is called the CANFLEX<sup>®</sup> (CANDU Flexible) bundle and consists of 43 fuel pins containing about the same amount of uranium in weight as the 37-element bundle. Figure 1 shows a CANFLEX fuel bundle prior to its loading into the CANDU reactor at Point Lepreau nuclear station for demonstration irradiation. Unlike its predecessors, the fuel pins of a CANFLEX bundle are separated into two groups with different outer diameters. Each pin is equipped with innovative, patented, no-load-bearing heat-transfer-enhancement devices called the buttons. Previous analyses and tests focusing on separate effects concluded that the buttons provide a significant improvement in critical heat flux (CHF) with minimal effect on pressure drop, compared to other heat-transfer-enhancing devices. A similar conclusion was made when the dryout-power and pressure-drop measurements were compared between the 37-element and CANFLEX bundle strings cooled with Freon-134a flow. This implies that the critical channel power of the CANDU reactor can be further improved by replacing the current 37-element bundles with a string of CANFLEX bundles.

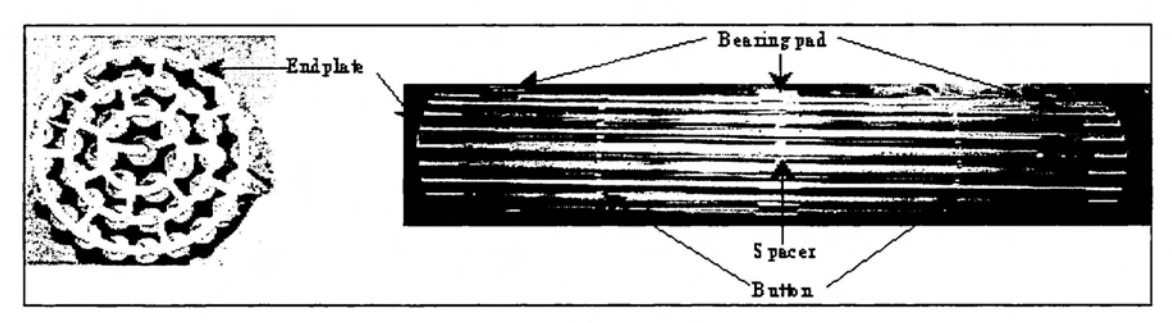


FIGURE 1: VIEWS OF A CANFLEX BUNDLE.

To confirm the improvement in critical channel power, a full-scale CANFLEX bundle test was recently completed to provide data on steady-state dryout power and fuel-string pressure drop. The test covered a wide range of flow conditions and three different flow tubes. This paper focuses primarily on data obtained at normal operating pressures with an axially non-uniform channel that had a maximum inside diameter 5.1% larger than a reference pressure tube. It presents the results of (i) an analysis of the data for dryout power, CHF and fuel-string pressure drop, and (ii) a comparison of these values between 37-element and CANFLEX bundle strings.

## 2. FULL-SCALE CANFLEX BUNDLE TESTS

Full-scale CANFLEX bundle tests were performed to obtain licensing data in the high-pressure steam-water loop at Stern Laboratories (Dimmick et al. 1999). The test string consisted of a 6-m-long, 43-element bundle simulator. The elements were constructed with Inconel tubes

<sup>(1)</sup> CANDU® and CANFLEX® are registered trademarks of Atomic Energy of Canada Limited (AECL).

of two different outer diameters (13.5 and 11.5 mm). Bundle segmentation was simulated with specially designed spool pieces that imitated the radial and cross webs of the endplate in a fuel bundle. Corresponding elements in the upstream and downstream bundles of the spool pieces were aligned axially. Appendages (i.e., spacers, bearing pads and AECL-patented non-load-bearing buttons) were spot-welded at various locations, as specified in the bundle design. Power was applied to the bundle string through Joule heating. The sheath thicknesses of the elements were varied along the axial length and from ring to ring. This provided accurate simulations of non-uniform radial and axial heat-flux distributions. The radial heat-flux distribution simulated a bundle with natural-uranium fuel, and the axial heat-flux distribution corresponded to a downstream skewed-cosine profile. A ceramic flow tube insulated the bundle string from the metal pressure boundary. Three different flow tubes were used in the test: one had a uniform inside diameter of 103.86 mm and the other two had axially varying inside diameters, with a peak of 107.29 mm and 109.16 mm (3.3% and 5.1% larger than the uniform tube). The uniform flow tube simulated a reference uncrept pressure tube, while others simulated pressure tubes with various degrees of diametral creep.

Figure 2 shows the set-up of the test station. Fourteen taps were installed along the test section; they were connected to differential-pressure (DP) cells to provide pressure-drop measurements over the bundle string. The taps at the inlet and outlet ends were also connected separately to other DP cells to measure the absolute pressures at those locations. K-type thermocouples and resistor temperature devices (RTDs) were used to monitor the fluid temperature at the inlet and outlet ends. The inside surface temperature of the heated sheath was measured with thermocouple-slider assemblies located inside the element. The sliders in all elements were moved axially and rotated at various locations to map out the surface-temperature distributions. Dryout occurrence was assumed for a sharp surface-temperature rise of about 5°C from the nucleate-boiling temperature. Details of the experimental set-up and test procedure are described in Dimmick et al. (1999).

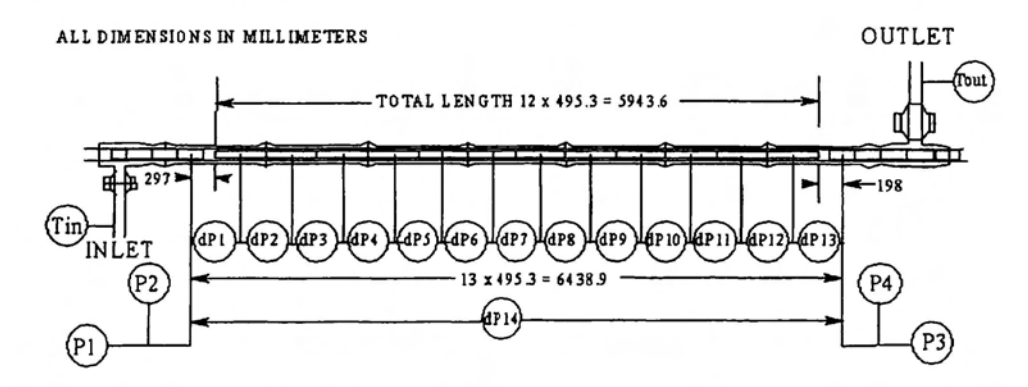


FIGURE 2: A SCHEMATIC DIAGRAM OF THE TEST STATION IN THE HIGH-PRESSURE STEAM-WATER LOOP AT STERN LABORATORIES.

A wide range of steam-water flow conditions was covered in the CHF experiment: an outlet-pressure range from 6 to 11 MPa, a mass-flow-rate range from 7 to 25 kg/s, and an inlet-fluid-temperature range from 200 to 290°C. The majority of the data are directly relevant to analyses

of the regional overpower trip (ROPT) set point in the reactor. In addition, single-phase and two-phase pressure-drop tests were performed at lower pressures and fluid temperatures, as well as at higher mass-flow rates. These data corresponded closely to those previously obtained with a simulated string of 37-element bundles at the same test facility.

# 3. DRYOUT POWER FOR THE CANFLEX BUNDLE STRING

The dryout power represents the total power applied to the bundle string at which the onset of intermittent dryout (OID) occurs. This corresponds to only a single point at the sheath of an element, where the liquid film has broken down, while a continuous liquid contact is maintained at the remaining surfaces of the bundle string. Because of the high heat-transfer rate due to convection (at high flow velocity) and conduction (from the dry spot to the surrounding wet area), a gradual temperature rise is associated with this type of dryout.

Figure 3 illustrates the variation in dryout power with inlet-fluid temperature and mass-flow rate at a constant outlet pressure of 11 MPa. Similar to the trends observed in tubes and 37-element bundles, the dryout power increased with decreasing inlet-fluid temperature and increasing mass-flow rate. Overall, the trends of dryout power followed a linear variation with these flow parameters over the test conditions. Several repeat points were obtained at various stages of the experiment (as indicated with multiple points at the same flow conditions). As shown in Figure 3, the repeatability of the measurements (multiple points at the same conditions) was excellent in the experiment. At conditions of interest (i.e., a mass-flow rate of 21 kg/s and an inlet-fluid temperature of 265°C), the dryout power for the CANFLEX bundle string was about 7.7 MW.

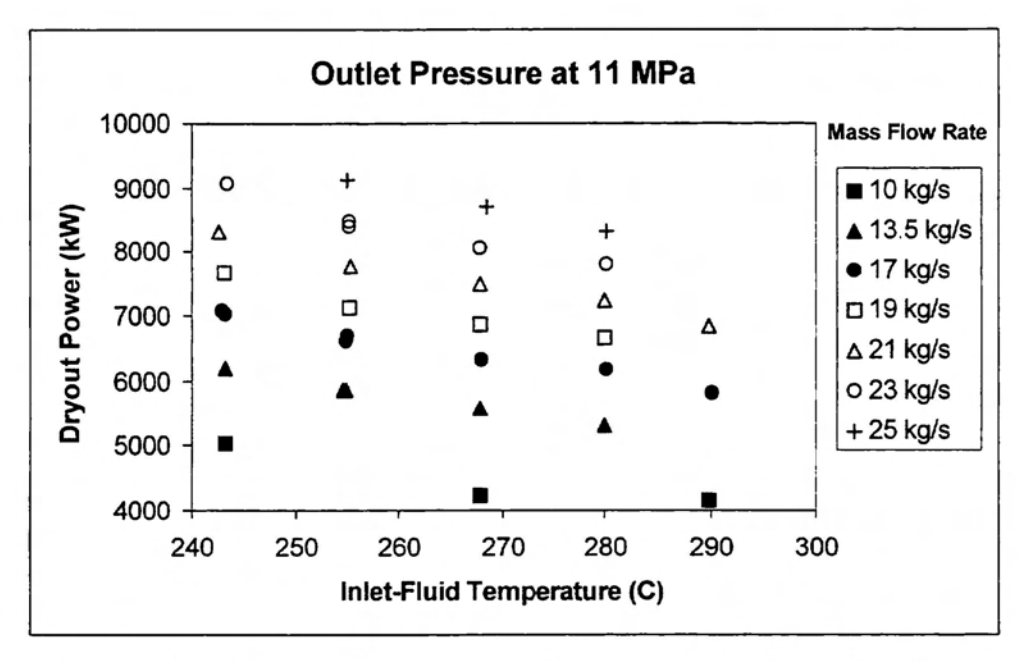


FIGURE 3: DRYOUT-POWER MEASUREMENTS FOR A CANFLEX BUNDLE STRING.

#### 4. CHF FOR THE CANFLEX BUNDLE STRING

The evaluation of critical channel power using a system code requires an accurate CHF correlation. Currently, there are three types of CHF correlation, based on local heat flux, boiling-length-average (BLA) heat flux, or critical quality. Overall, the BLA CHF correlation provides the best prediction accuracy in both CHF and dryout location for various types of channels.

The concept of boiling length was introduced by Bertoletti et al. (1964) to account for the effect of axial heat-flux distribution on CHF over the annular film-dryout region in tubes. Strictly speaking, the boiling length is measured from the onset-of-nucleate-boiling (ONB) point to the location of interest. However, due to the uncertainty in predicting the ONB point, the saturation point has traditionally been assumed to be the initiating point for flow in tubes. Furthermore, the dryout quality is often much larger than the qualities at either the ONB or saturation points (i.e., the boiling length is much greater than 0), and hence the impact of the assumption is reduced.

The traditional approach, as used in tube flow, to initiate boiling length from the saturation point is inappropriate for analyses based on the cross-sectional average flow conditions in a tightly spaced bundle. Imbalances in flow and enthalpy distributions in the bundle have led to the initiation of boiling (i.e., ONB point) at highly subcooled flow conditions (cross-sectional average values). These imbalances increase with increasing bundle eccentricity from the concentric position; a portion of flow diverges to the open area, bypassing the heated bundle. Hence, the assumption of a small difference between the ONB and saturation points is no longer justified, and the boiling length must be redefined.

In the CHF analysis for a 37-element bundle string, Leung et al. (1996) defined the boiling length from the onset-of-significant-void (OSV) point to the location of interest. The OSV point was determined from the pressure distribution based on the pressure-drop measurements at each set of inlet-flow conditions. The determination of the OSV point in a CANFLEX bundle string is described in Section 6. Leung et al. (1996) employed the OSV point rather than the ONB point because the pressure-drop data covered a much wider range of conditions than the surface-temperature measurements. Furthermore, the difference between the ONB and OSV points was observed to be small in the 37-element bundle string (Fortman et al. 1999).

Local and BLA CHF values were evaluated with the dryout-power measurements and axial heat-flux distribution. The BLA CHF is calculated with

$$CHF_{BLA} = \frac{1}{z_{DO} - z_{OSV}} \int_{z_{osv}}^{z_{DO}} q_{local} dz$$

where  $z_{DO}$  and  $z_{osv}$  are the locations at the dryout and OSV points, respectively,  $q_{local}$  is the local heat flux in W/m², and z is the axial distance in metres. Figure 4 compares the CHF values evaluated with either the local or BLA approach. The variation among the BLA CHF values is much less than that for the local CHF values with increasing dryout quality. Therefore, the BLA CHF values provide a better correlation than the local CHF values.

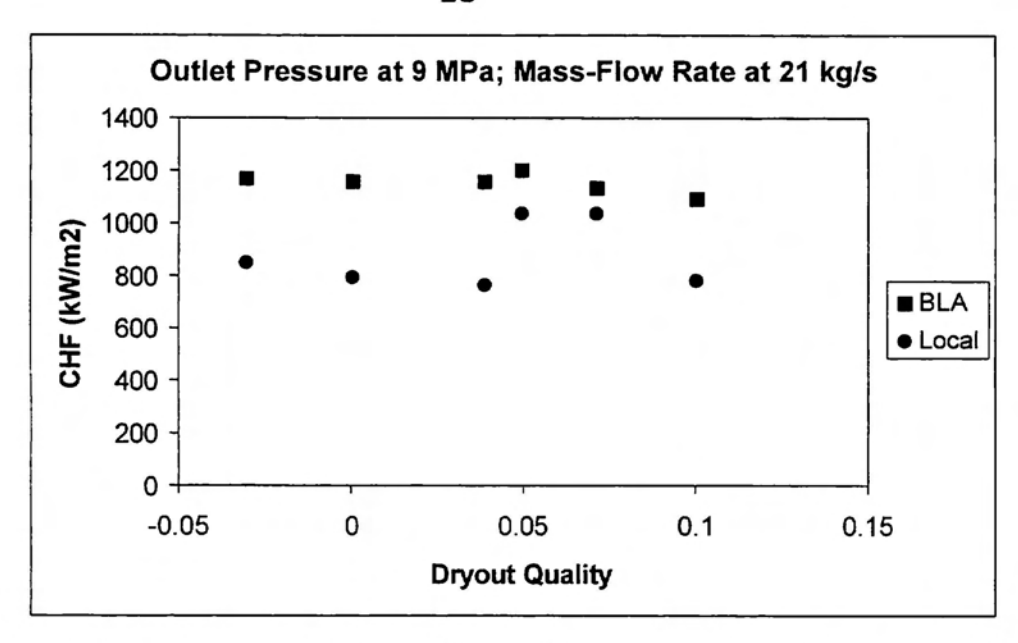


FIGURE 4: DIFFERENCES IN CHF BETWEEN THE BLA AND LOCAL APPROACHES.

Figure 5 compares the BLA CHF values for the CANFLEX bundle string at various dryout qualities and mass-flow rates. In general, the BLA CHF increases with decreasing dryout quality and increasing mass-flow rate. The same trend was observed in data obtained with tubes and the 37-element bundle string. As indicated in Figure 5, a number of data were obtained at the cross-sectional-average subcooled conditions (negative thermodynamic quality). Based on the current BLA approach, however, the data follow the same trend exhibited in the saturated dryout data. With respect to dryout quality, the variation of BLA CHF is larger at low mass-flow rates than at high mass-flow rates.

The BLA CHF values obtained at the outlet pressure of 9 MPa exhibit the same trends as those at 11 MPa (Figure 6). However, all data points, but one, lie at the saturated conditions. The trend of BLA CHF values with respect to dryout quality is similar for various mass-flow rates.

#### 5. PRESSURE DROPS OVER THE CANFLEX BUNDLE STRING

Pressure drops were measured with DP cells connected to taps installed along the CANFLEX bundle string (see Figure 2). They were used to establish the pressure distribution and hydraulic parameters (such as friction factor in single-phase flow, OSV and two-phase multiplier in two-phase flow). The distance over neighboring taps was equivalent to a bundle length (i.e., 0.495 m), and hence effects due to skin friction, bundle junction, mid-spacer plane, button plane and bearing-pad plane could not be isolated. Figure 7 illustrates the measured pressure distribution along the unheated bundle string. The non-linear variation of pressure is caused by the change in the flow-tube diameter with axial distance.

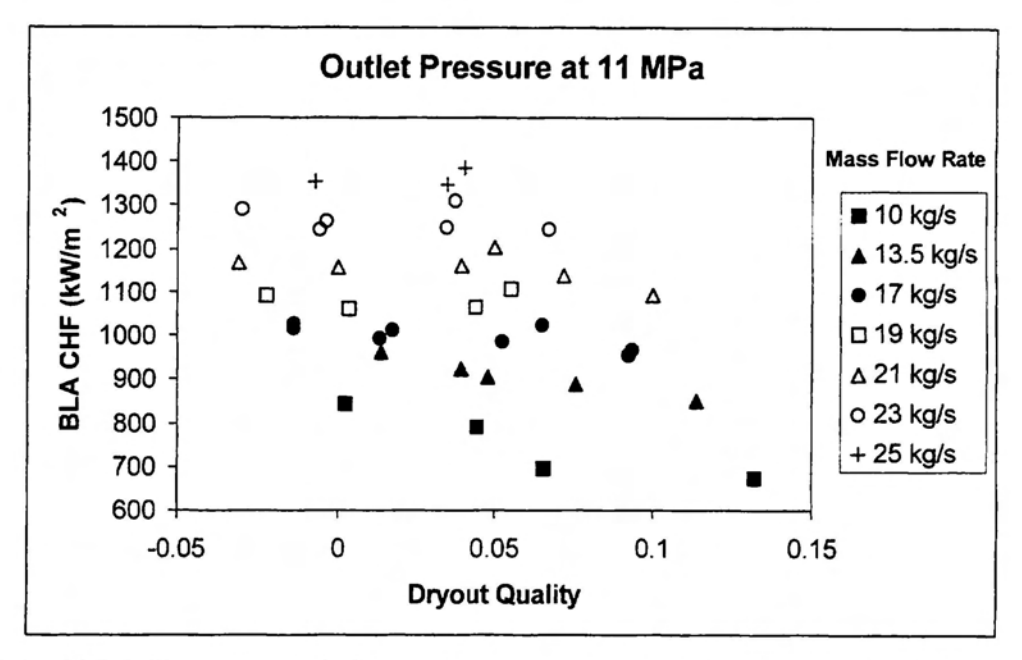


FIGURE 5: CALCULATED BLA CHF VALUES FOR THE CANFLEX BUNDLE AT AN OUTLET PRESSURE OF 11 MPA.

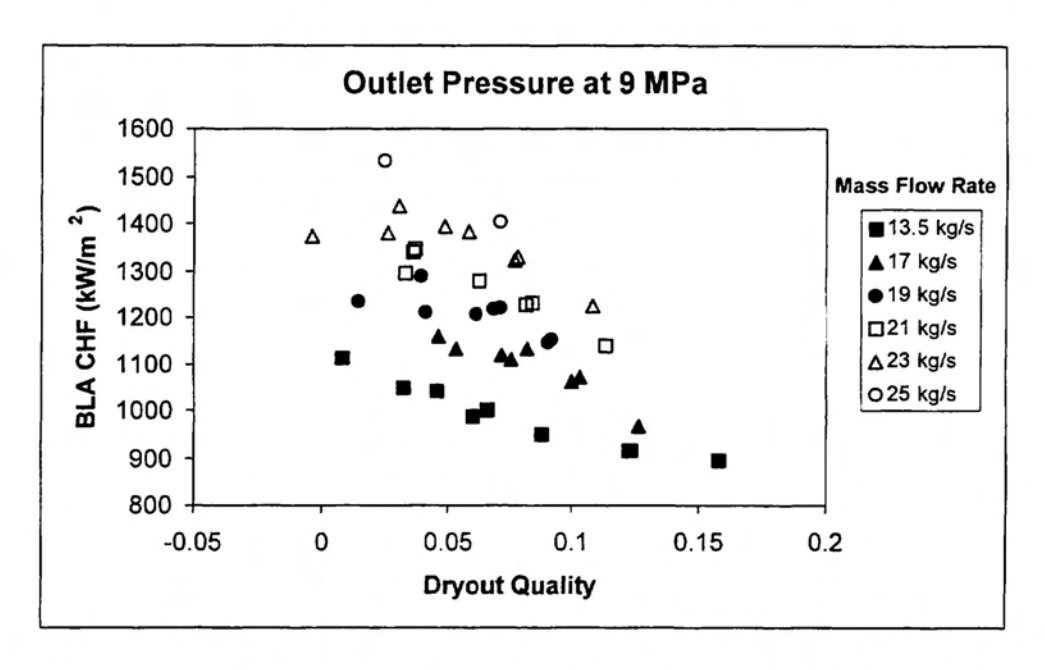


FIGURE 6: CALCULATED BLA CHF VALUES FOR THE CANFLEX BUNDLE AT AN OUTLET PRESSURE OF 9 MPA.

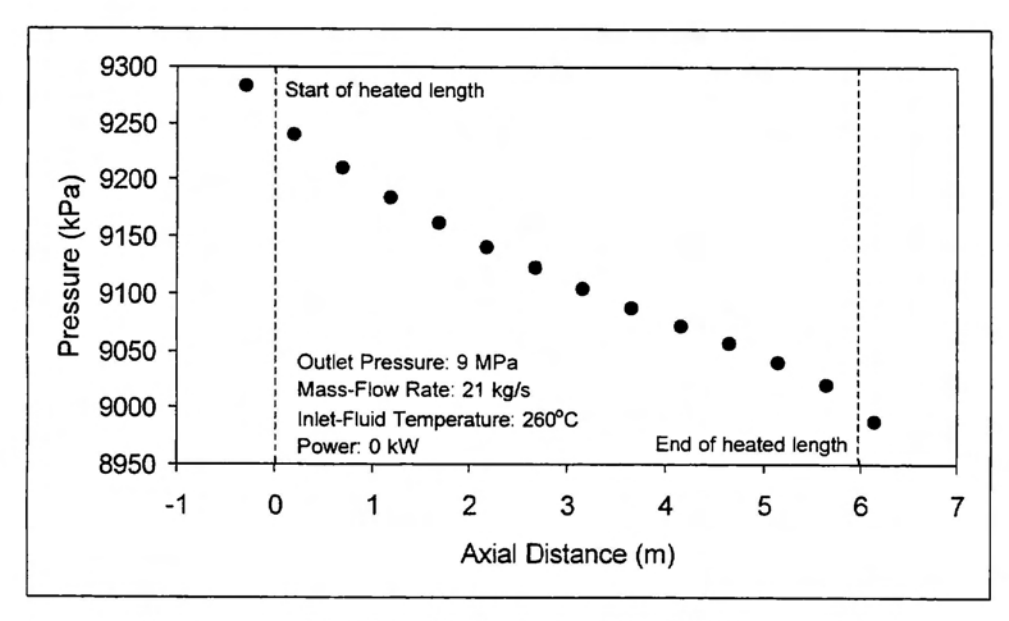


FIGURE 7: PRESSURE DISTRIBUTION ALONG THE UNHEATED BUNDLE STRING.

Figure 8 shows the axial pressure drops over various portions of the bundle string with reference to the outlet pressure tap at several power levels. The pressure-drop trend at low powers (i.e., 986 and 1972 kW) appears to be independent of the heating effect and follows closely the pressure distribution shown in Figure 7. This signifies that only single-phase liquid was flowing inside the channel and that boiling was suppressed. The channel pressure drop increased with increasing power and the pressure distribution varied strongly at the downstream end where boiling was encountered.

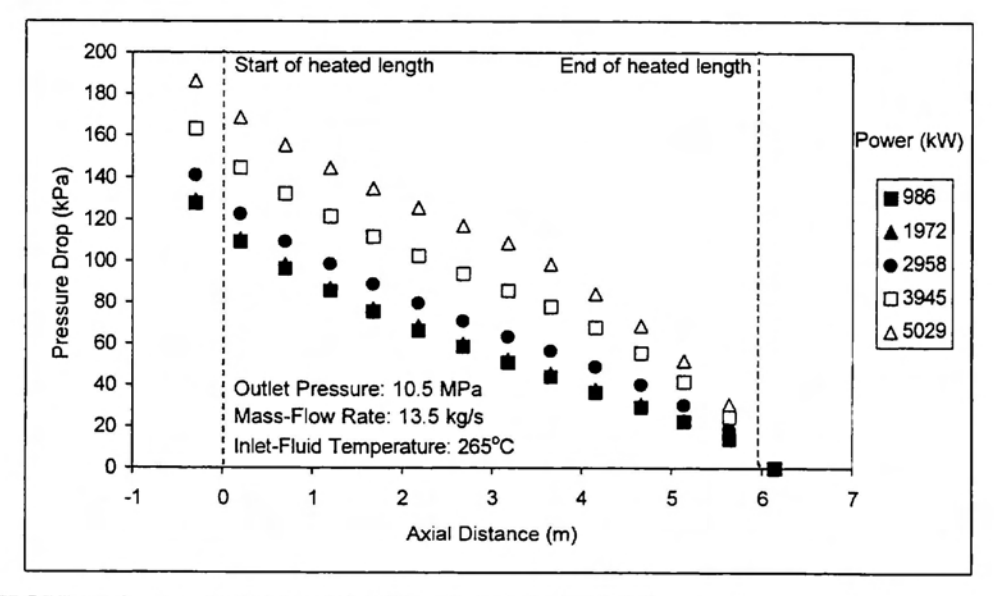


FIGURE 8: PRESSURE DROPS ALONG THE HEATED BUNDLE STRING.

# 6. ONSET OF SIGNIFICANT VOID IN A CANFLEX BUNDLE STRING

The OSV is often assumed to be the transition point between single-phase and two-phase flows. This is different from the ONB point, where bubbles are sustainable at the near-wall region only and would collapse when departing from the heated surface. While the pressure drop increases slightly at the region between the ONB and OSV points, the increase becomes considerably larger beyond the OSV point. Therefore, the OSV point is often determined from the pressure distribution along the channel. In a uniform channel, the single-phase pressure drop varies linearly, while the two-phase pressure drop varies non-linearly, with axial distance. Hence, the location at which the pressure gradient changes is considered to be the OSV point. In an axially non-uniform channel (i.e., varying flow area with distance), however, both the single-phase and two-phase pressure drops vary non-linearly and the turning point is difficult to establish (see Figure 8).

Leung and Hotte (1997) derived a single-phase pressure-drop model for CANDU fuel bundles, which was based primarily on correlations developed for simple channels (such as tubes and annuli). The model was validated against data obtained with both 4-rod and 37-rod bundle strings. It was used to calculate the single-phase pressure drop over the CANFLEX channel. By subtracting the predicted single-phase pressure drops from the measurements, the pressure drop over the single-phase region was eliminated, while the pressure variation over the two-phase region maintained a non-linear relation with axial distance. Figure 9 illustrates the modified pressure distribution along the CANFLEX bundle string. A slight variation in pressure with axial distance is still shown in the single-phase region; it is caused by the uncertainty in the pressure-drop model. Nevertheless, the transition between single-phase and two-phase flow is identified in the figure. Two polynomial equations were optimized separately with the data over the two pressure-drop regions. The OSV point was determined by solving these equations and locating the intersecting point.

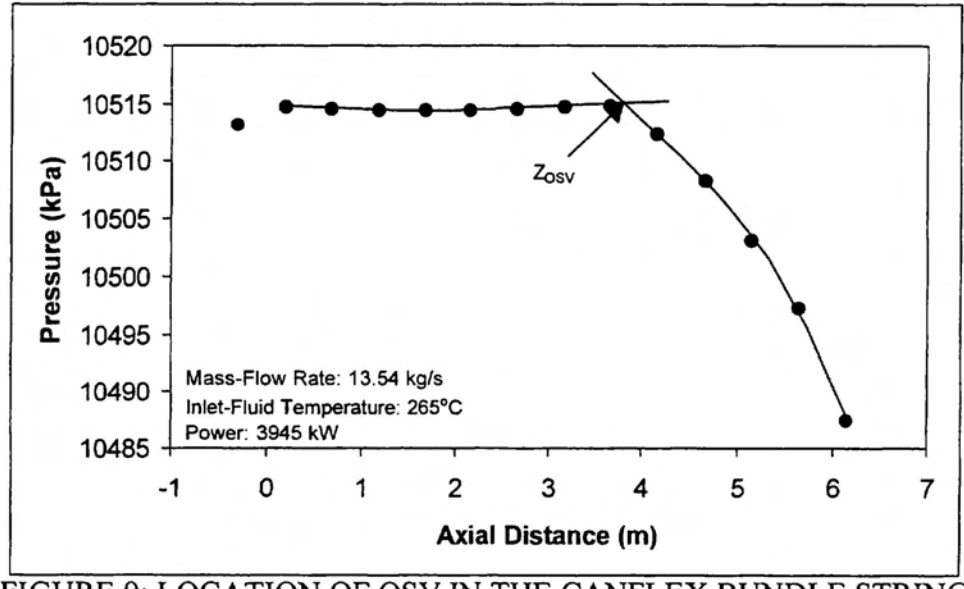


FIGURE 9: LOCATION OF OSV IN THE CANFLEX BUNDLE STRING.

# 7. COMPARISONS OF VARIOUS PARAMETERS BETWEEN CANFLEX AND 37-ELEMENT BUNDLE STRINGS

A similar experiment was previously completed with a simulated 37-element bundle string in the same test facility at Stern Laboratories. It covered a similar range of flow conditions and provided measurements on dryout power and pressure drop. Due to its proprietary nature, only a relative comparison of data between CANFLEX and 37-element bundles is presented here.

Figure 10 shows the dryout-power enhancement of the CANFLEX bundle string (i.e., the ratio of dryout power between CANFLEX and 37-element bundle strings) at similar inlet-fluid conditions. The dryout power for the 37-element bundle string is calculated with an optimized equation derived from the database. The overall average optimization error is 0.09% and the root-mean-square (rms) error is 3.29% for 86 data points. As Figure 10 shows, the dryout power is systematically higher for the CANFLEX bundle string than the 37-element bundle string. On average, the enhancement is about 17% for all data points. The effects of the inlet-fluid temperature and mass-flow rate on the enhancement are small over the present range, but a minor effect of pressure seems to be noticeable. The enhancement is slightly larger for data at 11 MPa than at 9 MPa.

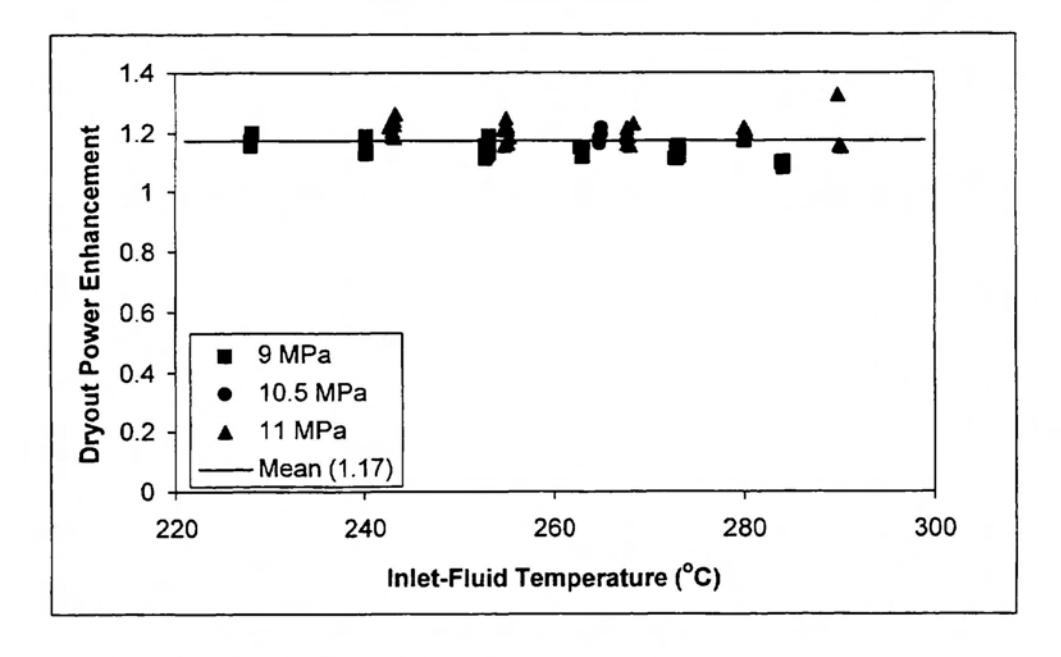


FIGURE 10: DRYOUT-POWER ENHANCEMENT FOR THE CANFLEX BUNDLE STRING INSIDE AN AXIALLY NON-UNIFORM CHANNEL WITH A MAXIMUM DIAMETER OF 5.1% GREATER THAN THE REFERENCE VALUE.

Figure 11 compares the pressure-drop characteristics between the CANFLEX and 37-element bundle strings at similar inlet-flow conditions and power (i.e., the same rate in enthalpy rise over the channel). Overall, the pressure-drop characteristics are similar for both bundle strings. A slightly higher fuel-string pressure drop is shown for the CANFLEX bundle string, and the

difference is about 2.1%. This is probably caused by the uncertainty in the simulation of the bundle junction and appendages.

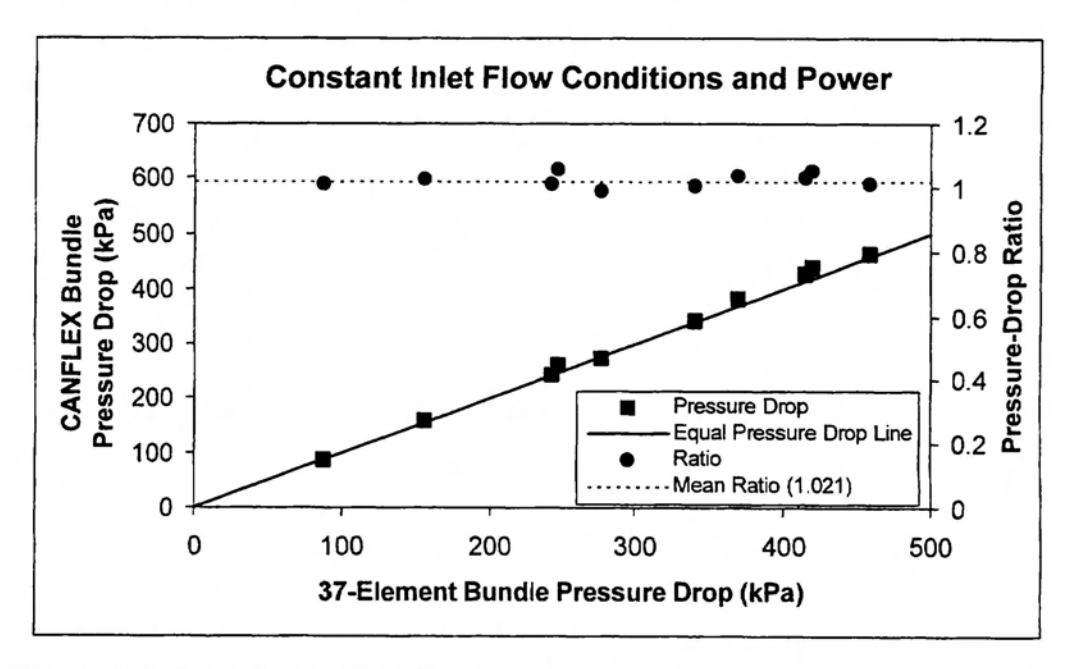


FIGURE 11: COMPARISON OF PRESSURE-DROP CHARACTERISTICS BETWEEN THE CANFLEX AND 37-ELEMENT BUNDLE STRINGS.

## 8. CONCLUSIONS AND FINAL REMARKS

- A set of data on dryout power and pressure drop has been obtained with a CANFLEX bundle string. The data are consistent and follow established parametric trends with various flow parameters.
- Local and BLA CHF values have been calculated with the dryout-power data.
- The OSV point has been determined using the pressure-drop measurements along the CANFLEX bundle string at various flow conditions.
- The dryout-power data are higher for the CANFLEX bundles than for the 37-element bundles. On average, the enhancement is about 17% for the range of conditions of interest at the same inlet-fluid temperature.
- The overall pressure drop is about the same for both bundle strings (the fuel-string pressure drop for the CANFLEX bundle is similar to that for the 37-element bundle at the same flow conditions and power).

# 9. REFERENCES

BERTOLETTI, S., GASPARI, G.P., LOMBARDI, C., PETERLONGO, G. AND TACCONI, F.A., "Heat Transfer Crisis With Steam-Water Mixtures", CISE-R-99, 1964.

DIMMICK, G.R., INCH, W.W.R., JUN, J.S., SUK, H.C., HADDALLER, G., FORTMAN, R. AND HAYES, R., "Full-Scale Water CHF Testing of the CANFLEX Bundle", Paper accepted for presentation at the 6<sup>th</sup> Int. Conf. on CANDU Fuel, Niagara Falls, Ontario, Canada, Sept. 26-30, 1999.

FORTMAN, R.A., HAYES, R.C. AND HADALLER, G.I., "37-Element CHF Program: Steady-State CHF, Transient CHF and Post-Dryout Tests with Uniform and Diametral Crept Flow Tubes", Unpublished proprietary report of the CANDU Owners Group (COG), 1999.

LEUNG, L.K.H., GROENEVELD, D.C. AND HOTTE, G., "Prediction Method To Account For The Effect Of Pressure-Tube And Diametral Creep On Critical Heat Flux And Pressure Drop For A 37-Element Bundle String", Proc. of the 19<sup>th</sup> CNS Simulation Symposium, Hamilton, Ontario, October 16-17, 1996.

LEUNG, L.K.H. AND HOTTE, G., "A Generalized Prediction Method For Single-Phase Pressure Drop In A String Of Aligned CANDU-Type Bundles", Proc. of the 20<sup>th</sup> CNS Simulation Symposium, Niagara-on-the Lake, Sept. 7-9, 1997.

# 10. ACKNOWLEDGEMENT

The authors would like to thank the test engineers at Stern Laboratories for performing the experiment and providing the experimental data.